Paul Stanley Bookout

Marshall Space Flight Center (MSFC)
Structural Analysis Division, ED23
AL 35812, USA

Statistically Generated Weighted Curve Fit of Residual Functions for Modal Analysis of Structures

A statistically generated weighting function for a second-order polynomial curve fit of residual functions has been developed. The residual flexibility test method, from which a residual function is generated, is a procedure to modal test large structures in a free–free environment to measure the effects of higher order modes and stiffness at distinct degree of freedom interfaces. Due to the present damping estimate limitations in the modal parameter evaluation (natural frequencies and mode shapes) of test data, the residual function has regions of irregular data, which should be a smooth curve in a second-order polynomial form. A weighting function of the data is generated by examining the variances between neighboring data points. From a weighted second-order polynomial curve fit, an accurate residual flexibility value can be obtained. The residual flexibility value and free–free modes from testing are used to improve a mathematical model of the structure, which is used to predict constrained mode shapes.

INTRODUCTION

Dynamically correlating a mathematical model with test results requires a modal test of the physical structure. The type of modal testing performed depends on the structure and the type of interfacing the structure has with its environment. The two most commonly performed modal tests are the free–free and fixed-base tests. For structures with constrained (fixed) interfaces, historically the fixed-base modal test was performed. Fixed-base testing has many drawbacks for large structures such as interface simulation and cost. Extreme difficulties arise when trying to simulate the interfaces between the structure and its environment when only selected degrees of freedom (DOF) are to be constrained. The cost involved in design and construction of a test stand can become prohibitive.

Due to simulation problems and economic pressures, alternative modal testing methods are being considered. Mass additive and residual flexibility testing methods are two such methods. The mass additive method involves the attachment of masses to the interface DOF, which helps to exercise the interface modes, aiding in constrained modes prediction. Admire et al. (1992a) and Coleman (1988) discuss the implementation of the method along with its advantages and disadvantages.

Received May 8 1995; Revised January 13 1997.
Shock and Vibration, Vol. 4, No. 4, pp. 211–222 (1997)
ISSN 1070-9622/97/$8.00

The residual flexibility modal testing method consists of measuring the free–free natural frequencies and mode shapes along with the interface frequency response functions (FRFs). Analytically, the residual flexibility method has been investigated in detail by MacNeal (1971), Martinez and colleagues (1984), and Rubin (1975), but it has not been implemented extensively for model correlation due to difficulties in data acquisition. In recent years improvement of data acquisition equipment has made the implementation of the residual flexibility method possible as in Admire et al. (1992b) and Klosterman and Lemon (1972). The residual flexibility modal testing technique is applicable to a structure with distinct points (DOF) of contact with its environment.

This article discusses the development of a statistically generated weighted curve fit to assist in the analysis of the residual flexibility test data. First, a brief analytical discussion is presented, followed by an explanation of the generation of the residual function from test data and the implementation of the statistically generated weighted curve fit to extract the residual terms. The residual flexibility method is then applied to a simple beam with a trunnion type interface and a space shuttle pallet simulator. The residual terms are then compared to a mathematical model taken as the exact answer, and percentage errors are presented.

RESIDUAL FLEXIBILITY ANALYTICAL APPROACH

The residual technique was first developed by MacNeal (1971) and incorporates the use of the higher frequency mode effects (residual modes) that are not directly used in the analysis to improve the reduced mathematical model. MacNeal statistically derives the displacement influence coefficient matrix, G, associated with the free coordinates, G_{cc}, and the redundant support coordinates, G_{ss}, for the determinate restrained boundary DOF, which is given by

$$G = \begin{bmatrix} G_{cc} & G_{cs} \\ G_{cs}^T & G_{ss} \end{bmatrix}, \tag{1}$$

where G_{cs} is the coupling of the redundant support and free coordinates.

MacNeal (1971) further defines the displacement influence coefficient matrix with an all boundary DOF restrained as

$$\overline{G}_{cc} = G_{cc} - G_{cs} G_{ss}^{-1} G_{cs}^T. \tag{2}$$

Next, casting the modal representation in a manner similar to the displacement influence coefficient matrix, Eq. (1), gives

$$G_{cc}^m = \Phi_{ci} - K_i^{-1} \Phi_{ci}^T, \tag{3}$$

where the Φ_{ci} term contains the eigenvectors at the connection point and K_i is the corresponding stiffness matrix. Subtracting Eq. (3) from Eq. (2) produces the residual flexibility matrix

$$G_{cc}^r = \overline{G}_{cc} - G_{cc}^m. \tag{4}$$

This approach is difficult to implement because of the way it was derived. MacNeal (1971) only makes use of the residual stiffness and neglects the mass and damping terms.

Rubin (1975) starts with the same statics approximation as MacNeal (1971), but formulates the residual flexibility in a different way. The statics approximation for a discrete system is written as

$$U_f^{(1)} = GF, \tag{5}$$

where $U_f^{(1)}$ is the displacement matrix of the flexible body, F is the external force vector, and G is the flexibility matrix of the free body.

The flexibility matrix is defined as the inverse of the stiffness matrix, $G = K^{-1}$. For the unconstrained case, the stiffness matrix is singular and G cannot be computed directly. For the constrained case, G_c can be calculated from K_c (constrained stiffness), $G_c = K_c^{-1}$. G and G_c differ by the rigid-body inertia forces of the system. When the system is unconstrained, the system has elastic and rigid-body movement. The rigid-body movement of the system has inertia forces associated with its mass. When the system is constrained, the elastic motion of the system is present but the rigid-body movement is missing. A way to incorporate the free-body inertia into G_c is needed to produce an equivalent unrestrained flexibility matrix.

Rubin (1975) writes the displacement of the physical coordinates due to generalized rigid-body displacements as

$$U_R = \Phi_R Q_R, \tag{6}$$

with the differential equation relating the generalized rigid-body displacements to the external forces being

$$M_R \ddot{Q}_R = \Phi_R^T F, \tag{7}$$

where $M_R = \Phi_R^T M \Phi_R$ is the rigid-body generalized mass and M is the physical mass matrix. The sum of the external forces, F, and the inertia forces, F_i, can be expressed as

$$F + F_i = F - M\ddot{U}_{\mathrm{R}} = AF, \tag{8}$$

where

$$A = I - M\Phi_{\mathrm{R}}M_{\mathrm{R}}^{-1}\Phi_{\mathrm{R}}^T.$$

The constrained equation for the static approximation for a discrete system, where G_{c} is the constrained body flexibility matrix, is stated as

$$U_{\mathrm{c}}^{(1)} = G_{\mathrm{c}}(F + F_i) = G_{\mathrm{c}}AF. \tag{9}$$

Rubin (1975) further explains that this is an unusual statics problem where the flexibility matrix G_{c} is singular and in general nonsymmetric.

By adding certain generalized rigid-body displacements, Q_{R}' to the constrained displacement given in Eq. (9), the static approximation flexible body displacements can be written as

$$U_{\mathrm{f}}^{(1)} = U_{\mathrm{c}}^{(1)} + \Phi_{\mathrm{R}}Q_{\mathrm{R}}'. \tag{10}$$

Defining the $U_{\mathrm{R}}^{(1)}$ in a way that it is orthogonal to the rigid-body modes (i.e., removing any rigid-body contributions) gives

$$\Phi_{\mathrm{R}}^T M\big[U_{\mathrm{c}}^{(1)} + \Phi_{\mathrm{R}}Q_{\mathrm{R}}'\big] = 0. \tag{11}$$

Solving for Q_{R}', substituting into Eq. (10), and using the relationship $M_{\mathrm{R}} = \Phi_{\mathrm{R}}^T M\Phi_{\mathrm{R}}$, the free-body symmetric flexibility matrix, G, for the static approximation is

$$U_{\mathrm{f}}^{(1)} = GF, \tag{12}$$

where

$$G = A^T G_{\mathrm{c}}A$$

and A is given in Eq. (8). Note that G is singular because G_{c} is singular.

The second-order statics approximation is obtained by including the inertial and damping forces of the static approximation displacements in Eq. (9)

$$U_{\mathrm{f}}^{(2)} = G_{\mathrm{c}}A\big[F - M\ddot{U}_{\mathrm{f}}^{(1)} - C\dot{U}_{\mathrm{f}}^{(1)}F\big], \tag{13}$$

and in a similar way removing the rigid-body contributions,

$$U_{\mathrm{f}}^{(2)} = GF - H\ddot{F} - B\dot{F}, \tag{14}$$

where

$$\begin{aligned} H &= GMG, \\ B &= GCG, \end{aligned}$$

and H and B are the inertial and damping coefficient matrices, respectively. Note that the inertial and damping coefficients are calculated from pre- and postmultiplication of G found from the first-order approximation. In addition, H and B are symmetric because G, M, and C are symmetric.

At this point, the approximate displacement for the entire flexible body for static and second order are given by Eqs. (12) and (14), respectively. By removing the retained modes (measured modes) in the above equations, the residuals are obtained.

The residuals for the static equation are

$$U_{\mathrm{f}\rho}^{(1)} = G_\rho F, \tag{15}$$

where

$$G_\rho = G - G_N, \quad G_N = \Phi_N K_N^{-1}\Phi_N^T,$$

and the mode shape and generalized stiffness matrices of the retained modes are Φ_N and K_N, respectively. Similarly, the second-order formulation is expanded from the statics equation by including correction terms,

$$U_{\mathrm{f}\rho}^{(2)} = G_\rho F - H_\rho\ddot{F} - B_\rho\dot{F}, \tag{16}$$

where

$$\begin{aligned} H_\rho &= H - H_N, \quad H_N = G_N M G_N, \\ B_\rho &= B - B_N, \quad B_N = G_N C G_N. \end{aligned}$$

G_ρ is given in Eq. (15) and H and B are given in Eq. (14). In addition, by making use of modal orthogonality, the residual mass and damping can be computed by pre- and postmultiplying the full mass and damping matrices, respectively:

$$H_\rho = G_\rho M G_\rho, \tag{17}$$

$$B_\rho = G_\rho C G_\rho. \tag{18}$$

One now has the equations to compute the residual flexibility (stiffness), residual mass, and residual damping terms for a mathematical model of a structure. Note that Martinez et al. (1984) restated the equations to determine the residual terms in a form that is similar to the Craig–Bampton (1968) formulation. The Craig–Bampton formulation is used widely in coupled loads analysis.

RESIDUAL FLEXIBILITY MODAL TEST APPROACH

Modal testing of a structure is required for correlation of a mathematical model of the structure. A mathematical model correlated to a free–free modal test is not accurate enough to predict the constrained mode shapes, as discussed by Admite et al. (1992b). The model must also be correlated to at least the residual flexibility terms, which in this study represent the flexibility around the interface points. In this procedure, the determinations of the test-generated $H_{\rho a}$, $B_{\rho a}$, and $G_{\rho a}$, the residual mass, damping, and flexibility, respectively, are used for comparison to the mathematical model's residual terms found in Eq. (16) and Eq. (15).

The residual flexibility modal test consists of first measuring the free–free modes in the frequency range of interest. This includes the rigid-body modes. (In the analysis, the mathematical model's rigid-body modes can be used if the total mass and its distribution in the model are relatively accurate.) The measured free–free modes are used to correlate the global modes of the mathematical model that can be performed at a later time. The structure is then excited at the points where it interfaces with its environment (boundary or interface DOF).

Exciting each interface point individually, the response due to the excitation is measured at the same location and in the same direction as the excitation, producing a drive point FRF. Modal parameters (mode shapes and natural frequencies) are then extracted from the FRF obtained from the free–free modal test. Synthesized FRFs are generated from the modal parameters and then subtracted from the corresponding drive point test FRFs. The remaining functions are called the residual functions. The residual flexibility term is defined as the value of the residual function evaluated at zero frequency (a constant term in the curve fit equation that will be discussed in detail later). The residual mass is the curvature of the residual function (the second-order term in the curve fit equation) in the displacement or force domain. Finally, the residual damping (the first-order term in the curve fit equation) is equated to the damping obtained from the modal test. The residual terms are then compared to the corresponding theoretical residual terms. The mathematical model is modified to match the test results. Once the mathematical model is correlated to the free–free mode shapes and the residual terms, it can be used to predict the constrained mode shapes as Admire et al. (1992b) demonstrates on the Space Station Common Module Prototype, built by Boeing.

In this derivation, the residual terms will be extracted from the FRF in the displacement or force domain instead of the usual acceleration or force domain. Using the displacement or force domain allows easier recognition of the characteristics of the residual function and the residual flexibility term.

Y_a, the frequency response function matrix, is represented in the form,

$$U_a(\omega) = Y_a(\omega) F_a(\omega). \tag{19}$$

The elements of the main diagonal of $Y_a(\omega)$ are the drive point FRFs at each interface point and direction. One column of $Y_a(\omega)$ is the result of exciting one interface point and measuring the response at that point and all the other interface points and directions. $Y_a(\omega)$ can be thought of as a 3-dimensional matrix with 2 dimensions of the matrix defining the location and direction of a particular FRF. The third dimension along the ω axis represents the actual values of the FRFs. The FRFs are only measured in the frequency range of interest. The unmeasured range will produce the residual function.

The technique for obtaining the response functions is left up to the test engineer. Care must be taken to accurately measure the first antiresonance of the response function. An accurate determination of the first antiresonance is the governing factor in determining the residual flexibility term. The first antiresonance is the lowest frequency distinguishable characteristic of the FRF; and because the residual flexibility term is evaluated at zero frequency of the residual function, any shift in the first antiresonance significantly affects the residual flexibility term.

The modal parameters are extracted from the FRFs producing retained natural frequencies and mode shapes. These natural frequencies and mode shapes together with the rigid-body modes are subtracted from the corresponding FRF to produce the residual function coefficients, $Y_{\rho a}(\omega)$,

$$Y_{\rho a}(\omega) = Y_a(\omega) - \Phi_{\mathrm{R}a} Y_{\mathrm{R}} \Phi_{\mathrm{R}a}^T - \Phi_{Na} Y_N \Phi_{Na}^T, \tag{20}$$

where $\Phi_{\mathrm{R}a}$ and Φ_{Na} are the rigid-body and retained free–free modes, respectively, and

$$\begin{aligned} Y_{\mathrm{R}} &= -\frac{1}{\omega^2} M_{\mathrm{R}}^{-1}, \\ Y_N &= \Lambda_N^{-1} M_N^{-1}, \\ \Lambda_N &= -\omega^2 + i2\zeta_n \omega\omega_n + \omega_n^2. \end{aligned}$$

Y_{R} and Y_N are the modal dynamic flexibility matrices for classically damped modes. The rigid-body mass and retained elastic-body modal mass, M_R and M_N, respectively, are identity matrices if the modes are initially normalized to modal mass.

Once the residual function is determined, the residual terms (flexibility, mass, and damping) are extracted. A second-order form, similar to Eq. (16), is used to estimate the residual function,

$$Y_{\rho a}(\omega) = \omega^2 H_{\rho a} - i\omega B_{\rho a} + G_{\rho a}. \tag{21}$$

As can be seen, the residual function $Y_{\rho a}(\omega)$ is a complex number and the real and imaginary components can be separated. $Y_{\rho a}(\omega)$ is in the form,

$$Y_{\rho a}(\omega) = a + bi, \tag{22}$$

where

$$a = \text{Real}(Y_{\rho a}(\omega)), \qquad b = \text{Imag}(Y_{\rho a}(\omega)).$$

Equating Eq. (21) and Eq. (22) gives,

$$a + bi = (\omega^2 H_{\rho a} + G_{\rho a}) - i\omega B_{\rho a}. \tag{23}$$

Equating the imaginary components, the residual damping term is found to be

$$B_{\rho a} = -\frac{b}{\omega}. \tag{24}$$

The residual mass and flexibility are determined by equating the real components;

$$a = G_{\rho a} + \omega^2 H_{\rho a}. \tag{25}$$

Rewriting Eq. (25) in matrix form gives

$$a = AX, \tag{26}$$

where

$$A = \begin{bmatrix} 1 & \omega_1^2 \\ 1 & \omega_2^2 \\ \vdots & \vdots \\ 1 & \omega_N^2 \end{bmatrix}, \qquad X = \begin{bmatrix} G_{\rho a} \\ H_{\rho a} \end{bmatrix},$$

and N is the total number of data points. Solving for X gives

$$X = A^{-1}a, \tag{27}$$

the residual flexibility and the residual mass. Because A is not suqare, other solution methods must be implemented, such as the pseudoinverse, to determine the unknowns $G_{\rho a}$ and $H_{\rho a}$. These values are compared to the residual terms calculated from the mathematical model for correlation purposes.

LEAST-SQUARES CURVE FIT OF RESIDUAL FUNCTION

The determination of the residual terms (residual mass and flexibility) from the residual function requires a second-order polynomial curve fit of Eq. (25). The imaginary term (residual damping) was previously determined in Eq. (24) and is not included in the curve fit. If the subtraction of the synthesized FRF from the test (measured) FRF was clean (i.e., no irregular data regions), a direct curve fit could be accomplished for Eq. (27). When subtracting the synthesized FRF from the test FRF, the magnitudes of the peaks (damping terms) are required to be accurate to produce a smooth second-order curve. But due to the damping errors in the synthesized FRF, the resulting residual function has regions of irregular data. The errors in the synthesized FRF are attributed to the limitation in determining accurate damping terms when extracting the modal parameters from the test FRFs.

A theoretical residual function in the displacement or force domain has the characteristics of a relatively flat line in the lower frequencies and a slight upward curvature in the higher frequency range. These are the characteristics of a second-order equation with only the constant and second power terms [Eq. (25)]. Using these characteristics, a weighted curve fit of the residual function could be used to eliminate the irregular data. A method of determining the weighting function for the curve fit that eliminates any guesswork from the analyst is required.

As stated previously, the residual function is relatively flat at the lower frequencies, or in other words, the difference (variance) between adjacent data points is small. In the regions of irregular data, the variance between adjacent data points is large. When the variance is large between data points, its influence on the curve fit should be minimized. In addition, the data point pairs with small variance should have their influence increased. Because a large variance requires a small influence and small variance requires a large influence, the inverse of the variance is used to eliminate the regions of irregular data. By taking the inverse of the variance of adjacent data points, a weighting function, W, is generated:

$$W(j) = \frac{1}{s^2(j)} = \frac{n-1}{\sum_{i=j-\text{int}(n/2)}^{j+\text{int}[(n-1)/2]} (x_i - \overline{x})^2}, \tag{28}$$

where

$$j = \text{int}\left(\tfrac{n+2}{2}\right), \text{int}\left(\tfrac{n+2}{2}\right) + 1, \ldots, N - \text{int}\left(\tfrac{n-1}{2}\right),$$

$s^2(j)$ is the variance as defined by Miller et al. (1990), N is the total number of data points, n is the number of adjacent data points for which the variance is calculated, $\bar{x}$ is the mean of the n adjacent data points for each j, and int(#) is the integer part of # [i.e., $\text{int}(1.5) = 1$].

Forming W into a square matrix is accomplished by setting the main diagonal equal to the weighting function and all other terms equal to zero. The square matrix W must be $N \times N$ in size. When calculating the weighting function, the first and last few data points, depending on the value of n chosen, will not have a weighting value assigned. Forcing a value of zero at these points will make W be $N \times N$. This can be justified by the fact that at the extreme limits data acquisition equipment is not as accurate as in the middle range of the equipment, and the test generated residual function is not as accurate there either. Eliminating these points will have little influence on the curve fit. In the following sections this is demonstrated in the study on the beam with exaggerated data point elimination. In addition, only the weighting values of about two or four data points will be set equal to zero compared to about 250 total data points.

Premultiplying both sides of Eq. (26) by the weighting function matrix gives

$$Wa = WAX. \tag{29}$$

Multiplying both sides by A^T and solving for X yields

$$X = \left(A^T WA\right)^{-1} A^T Wa. \tag{30}$$

Because $A^T WA$ is a square matrix, the inverse can be computed directly. In this form there is no need to normalize the weighting function. The residual terms (residual mass and flexibility), which are contained in X, can be used to correlate the mathematical model.

APPLICATION TO BEAM WITH APPENDAGE

One of the simplest structures to model is a straight beam. A theoretical solution for the natural frequencies and mode shapes of an inrestrained (free–free) uniform beam is available from Blevins (1979). With the "exact" answer available, the mathematical model's elastic modes can be correlated. Once the model is correlated, the model is said to be exact. The mathematical model of the simple beam was correlated to have a frequency difference less than 0.5% for the first six modes and modal assurance criteria (MAC) values of 1.0. The MAC is an averaged value for the comparison of the mode shapes in the range from zero to one. A value of one indicates a high degree of similarity between mode shapes. The correlated model can be used as a baseline for methodology, program development, and test method evaluation.

For this study the beam structure was modified by attaching a trunnion simulator to one end (Fig. 1). The trunnion simulator was a brass rod with two aluminum plates attached on both ends. The plates were used to connect the brass rod to the beam and to attach the testing instruments. The trunnion simulator gives the beam a distinct stiffness change from the free–free beam. The mass of the trunnion simulator is small relative to the mass of the beam and does not affect the correlation to the solution of the theoretical uniform free–free beam.

Initially, the beam was tested in a free–free configuration and the elastic modes were compared to the mathematical model. The differences between natural frequencies for each of the six modes were less than 0.2% and the MAC values were all 1.0. The measurements and the modal parameter estimation (natural frequencies and mode shapes) of the free–free modal test were verified by these results.

By exciting the test structure at the point where it interfaces with its environment (the end of the brass rod) and measuring the response at the same location, a drive point FRF in the displacement domain was obtained. The modal parameters were computed for the first six natural frequencies, and a synthesized response function was generated. The first six natural frequencies in the maximum frequency range of 0–200 Hz were chosen arbitrarily.

For visual comparison, the drive point and synthesized FRFs are plotted together in Fig. 2. The frequency range has been extended to show the relationship between the measured frequencies and the first bending frequency of the trunnion, which occurs at 289 Hz. In an actual test, everything above the cutoff frequency would be unmeasured. The unmeasured region of the FRF is responsible for the residual curve. The subtraction of the test and synthesized response functions producing the residual function can be seen in Fig. 3. The characteristics of the theoretical residual function are apparent, but regions of irregular data are produced by modal parameter estimations.

A direct curve fit of the residual function was made. The curve fit did not converge on the underlying second-order characteristic curve. The irregular data are orders of magnitude higher than the underlying second-order characteristic curve, which does not let the curve fit converge. By stepping through the data points, a weighting value (inverse of variance) with

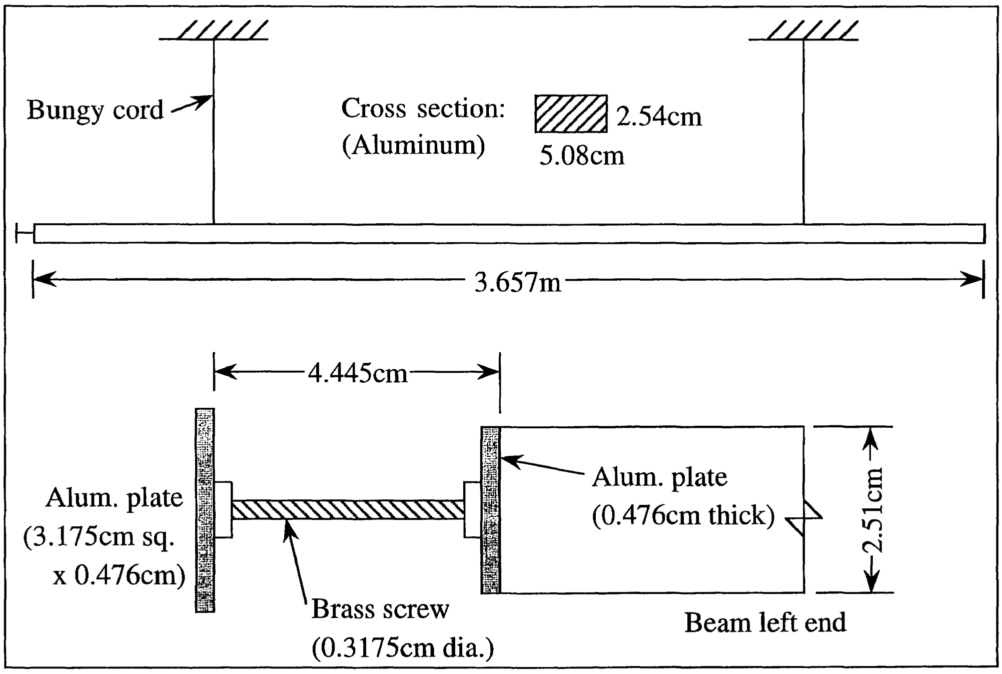

FIGURE 1 Beam with trunnion attachment test article.

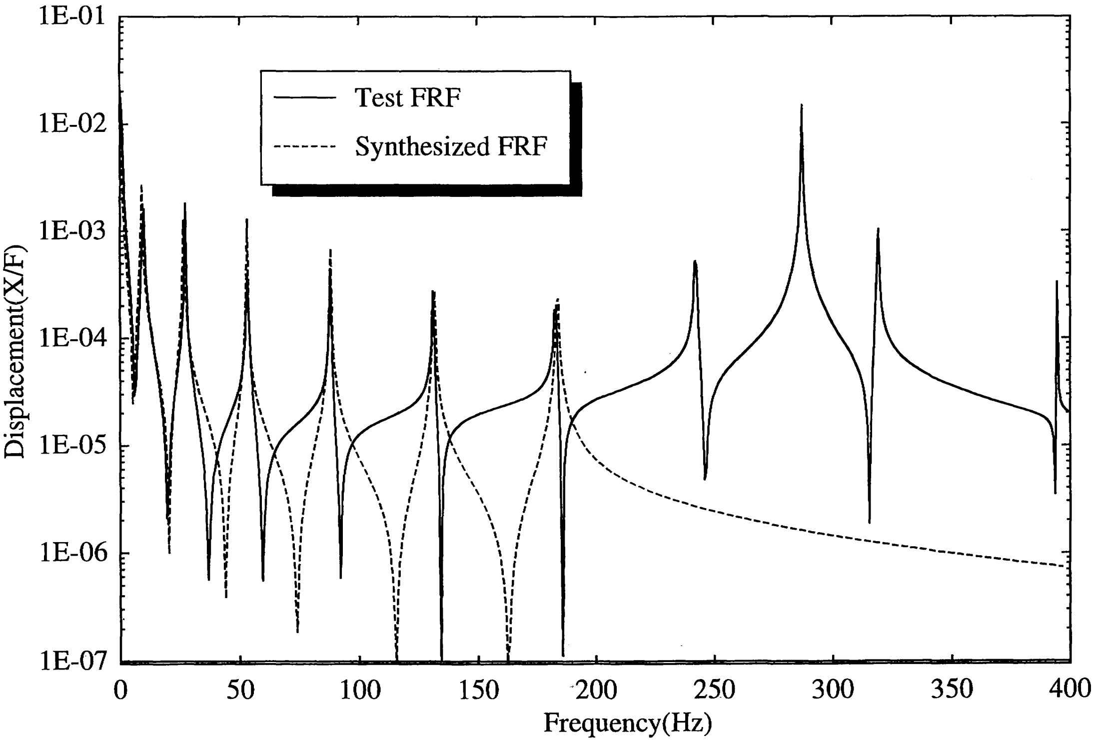

FIGURE 2 Overlay of test and synthesized drive point FRFs for beam.

respect to the neighboring data points can be calculated [Eq. (28)]. The neighboring data points were initially examined in sets of three. It can be seen in Fig. 4 that the weighting function has low values where the residual function has regions of irregular data. Another curve fit was performed using the statistically generated weighting function [Eq. (30)] and the results were highly accurate (Fig. 4).

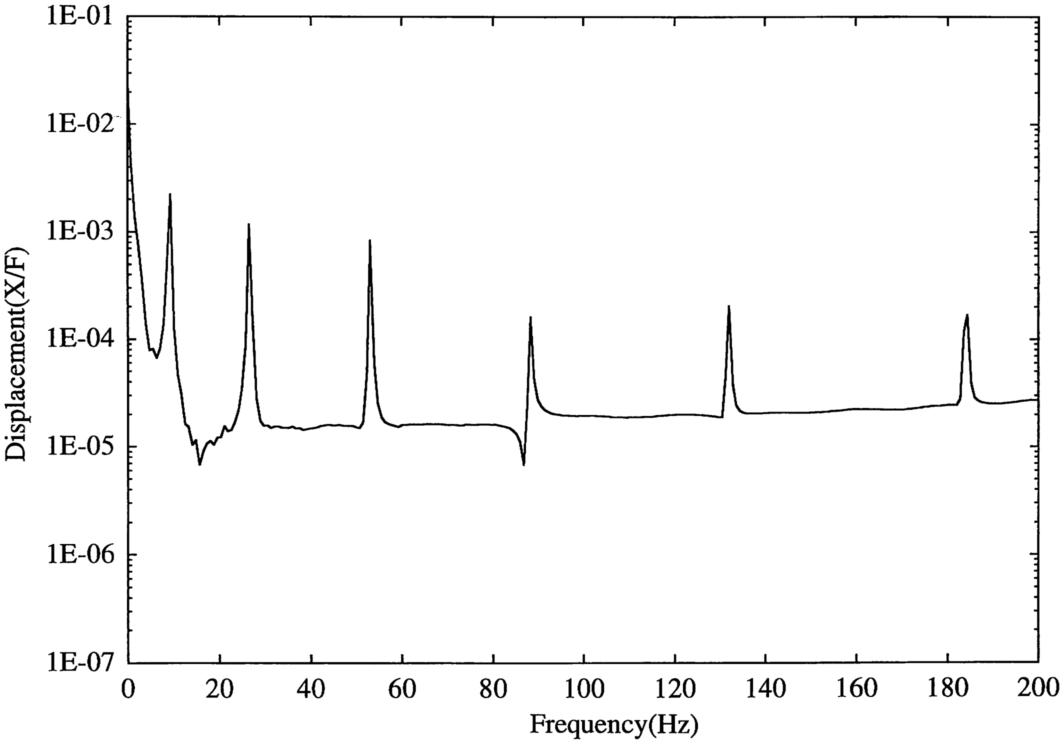

FIGURE 3 Residual function.

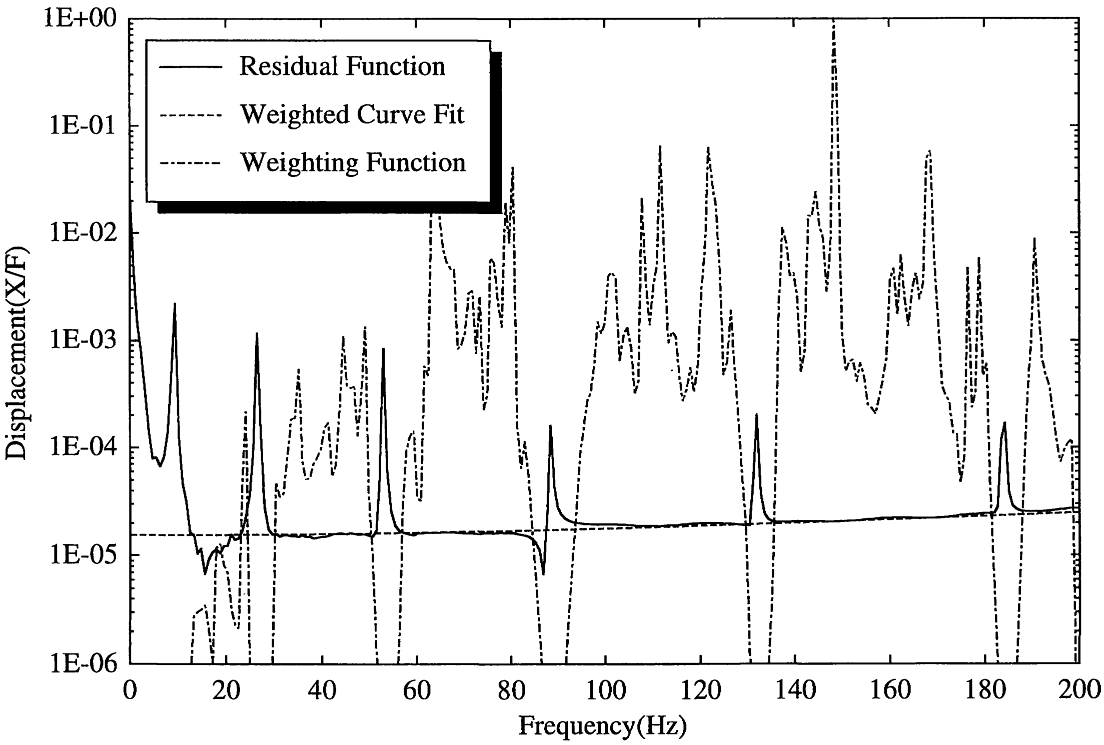

FIGURE 4 Weighted curve fit of residual function for beam.

The exact answers were obtained with Eq. (16). The same values can be obtained by following the test procedure in generating the residual function. The drive point FRF is generated by using the elastic modes of the model. The residual values of 1.6045e-5 for flexibility and 5.7540e-12 for mass were compared to the exact answer (mathematical model) and were found to have 0.81 and 18.44% error, respectively. In this research task being performed by the Marshall Space Flight Canter/NASA, the residual mass and damping terms were neglected in the correlation of the mathematical model due to the small magnitude of the mass terms compared to flexibility and inaccuracy of determining test damping. Further investigation of the use of these terms for model correlation is planned. However, the residual mass term is important in the curve fitting process due to the curvature of the residual function. To verify the process, additional weighting functions and curve fits were performed by varying parameters. The number of adjacent data points was changed to two and four along with the range of the data points for which the weighting functions were computed and applied (Table 1).

By varying the upper and lower frequency ranges, an evaluation of the effects of excluding data points in the curve fit process is examined. The changes in the percent error of the frequency range variation in Table 1 is insignificant. The comparison of the utilization of two, three, and four consecutive data points to generate the weighting function shows that a small change with three points produces the best results.

The larger error in the 2- and 4-point evaluation can be attributed to the distribution of the data point of the curve. For instance, if two consecutive data points staddle a peak (defines the peak) at equal heights, their variance may be low but their overall magnitude is greater then the characteristic curve. A high weighting value would be assigned which would produce an incorrect curve fit (i.e., residual flexibility value).

APPLICATION TO PALLET SIMULATOR

Once the method and programs have been verified on a simple structure (beam) with a known "exact" (theoretical) answer, the implementation on a more complex structure is performed. A frame structure (Fig. 5) has been designed and built to simulate a space shuttle cargo pallet. The fundamental mode distribution and trunnion modes of the frame structure are similar to a space shuttle cargo pallet.

A theoretical exact solution is not available for the pallet simulator. To obtain the closest model representation to the physical structure, the mathematical model (finite element model) is correlated to the elastic modes obtained from the modal test data. All the elastic modes up to the first bending mode of the trunnions are correlated. In an actual test, only a subset of the elastic modes (up to a prechosen cutoff frequency) would be used in the correlation. In this analysis, the first eight natural freuqencies are used in the determination of the residual values. Because the mathematical model is correlated through the 14 elastic modes, the use of the model to predict the residual terms of the first eight modes can be accomplished with confidence.

The pallet simulator was suspended by bungee cords in a free–free environment. The modal test was conducted using a random vibration shaker excitation in the three translational directions in sequence. The mathematical model was then correlated to the first 14 elastic natural frequencies and mode shapes. The difference between natural frequencies for each of the 14 modes were less than 0.95% and the MAC values were all 1.0. With a frequency difference less than 1% and MAC values of 1.0, an exact mathematical model is said to be obtained.

The drive point FRFs are measured at the points where the structure would connect (interface) with its environment (end of the trunnions). A hammer impact excitation was used to excite the structure with a data acquisition frequency range up to 100 Hz. If the shaker was attached to the end of the trunnion, mass and stiffness loading would occur due to the size of the trunnion and additional uncertainties in the data this would be imposed. The response function at the other interface points was acquired for each drive point excitation with a total of 144 FRFs obtained.

Examining one of the drive point FRFs, modal parameters (mode shapes and natural frequencies) were extracted for the first eight elastic modes. Using these eight modes, a synthesized FRF was generated. The synthesized and the drive point FRFs are plotted together (Fig. 6) for visual comparison. The frequency range in Fig. 6 has been extended to show their relationship. Subtracting the synthesized FRF from the drive point FRF, the residual function was generated (Fig. 7). It can be seen that a direct curve fit of the residual function would cause extreme divergence as in the beam's residual function curve fit.

A weighting function was generated using three consecutive data points (Fig. 7). Applying the weighted curve fit to the residual function, the residual flexibility and residual mass are found to be 7.6738e-6 and 5.6104-12, respectively (Fig. 7). The residual terms

Table 1. Residual Flexibility Curve Fitting Errors for Beam

Lower Freq.	Upper Freq.	2 Points	% Error	3 Points	% Error	4 Points	% Error
Exact		1.6165e-5	0.00	1.6165e-5	0.00	1.6165e-5	0.00
0	200	1.5761e-5	2.52	1.6035e-5	0.81	1.5833e-5	2.06
30	200	1.5757e-5	2.53	1.6035e-5	0.80	1.5835e-5	2.04
60	200	1.5771e-5	2.44	1.6225e-5	0.37	1.5865e-5	1.86
0	180	1.5758e-5	2.52	1.6066e-5	0.61	1.5888e-5	1.71
30	180	1.5758e-5	2.52	1.6067e-5	0.60	1.5890e-5	1.70
60	180	1.5772e-5	2.43	1.6268e-5	0.64	1.5923e-5	1.50

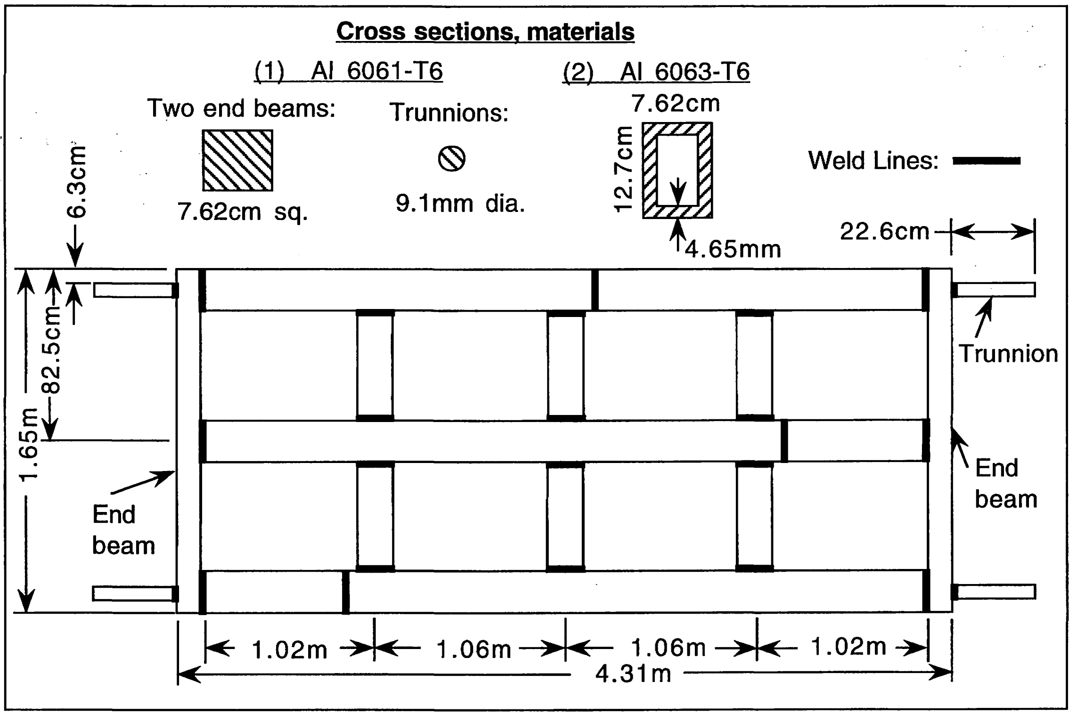

FIGURE 5 Space shuttle pallet simulator.

Table 2. Curve Fitting Errors of Pallet Simulator Residual Flexibility

Lower Freq.	Upper Freq.	2 Points	% Error	3 Points	% Error	4 Points	% Error
Exact		7.8707e-6		7.8707e-6		7.8707e-6	
0	100	7.5776e-6	3.72	7.6738e-6	2.50	7.6923e-6	2.27
20	100	7.6056e-6	3.37	7.6842e-6	2.37	7.7037e-6	2.12
40	100	7.8214e-6	0.63	7.9305e-6	0.76	7.9457e-6	0.95
0	90	7.2536e-6	7.84	7.5488e-6	4.09	7.5553e-6	4.01
20	90	7.3175e-6	7.03	7.5658e-6	3.87	7.5764e-6	3.74
40	90	7.7639e-6	1.36	7.9176e-6	0.60	7.9368e-6	0.84

from the exact mathematical model were computed and compared to the test generated residual terms with a test error of 2.50 and 1.36% for flexibility and mass, respectively. The number of consecutive data points and the frequency range for weighting function generation were changed to verify the curve fitting process (Table 2). A similar variation in the percent error was observed as in the beam results.

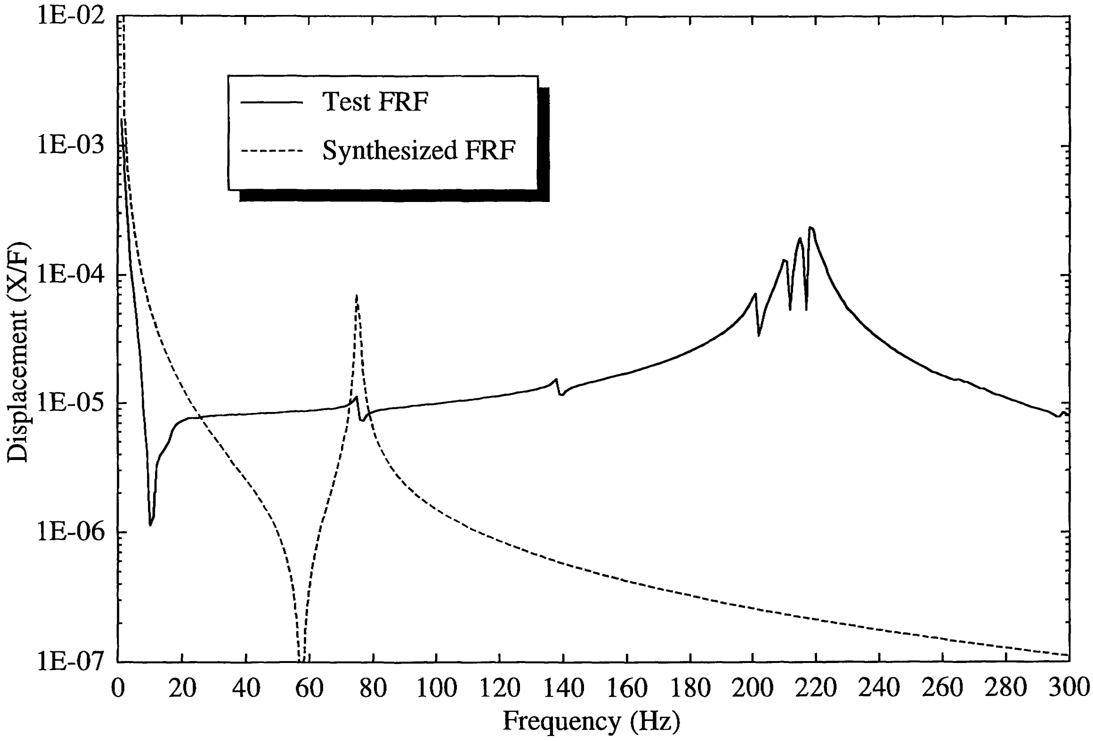

FIGURE 6 Overlay of test and synthesized drive point FRFs for pallet simulator.

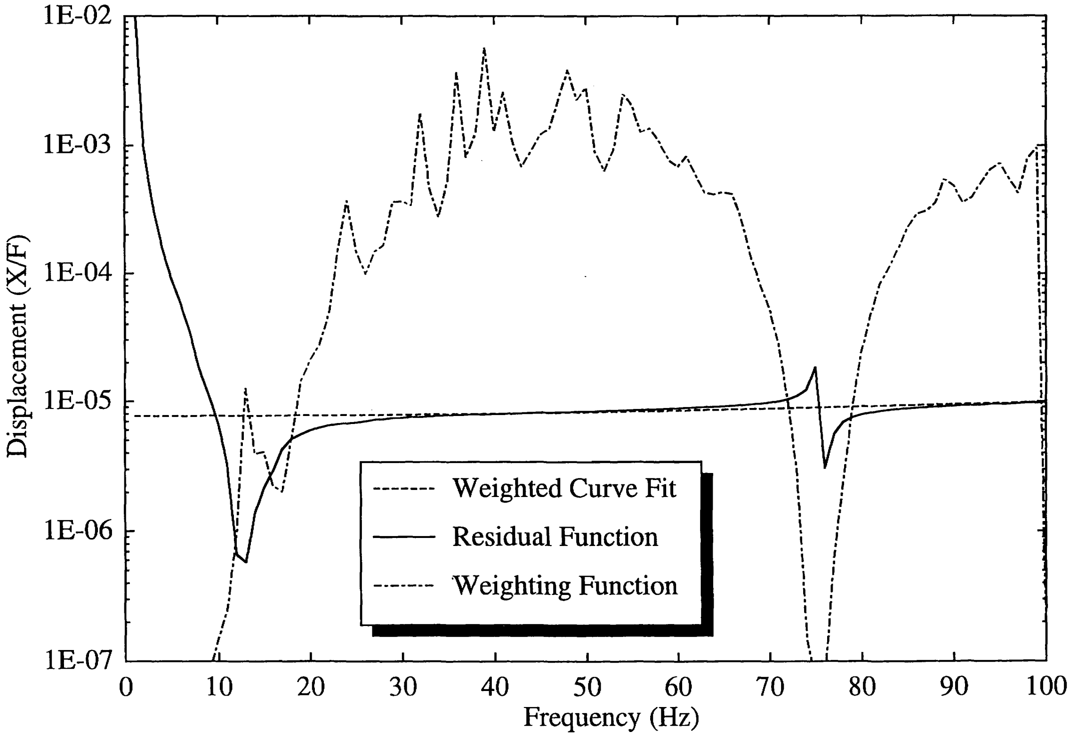

FIGURE 7 Weighted curve fit of residual function for pallet simulator.

CONCLUSION

An applicable least-squares curve fitting procedure using a statistically generated weighting function has been developed. This curve fitting procedure enables the accurate curve fitting of test-generated residual functions that contain regions of irregular data. The irregular data are the result of the inability to accurately evaluate the damping when extracting the modal parameters from the FRF during the modal testing process. Programs for calculating the residual terms from modal test data and a mathematical model (finite element model) have been written in MATLAB™. The curve fit of the drive point residual function for a beam with a trunnion type interface, retaining the first six elastic modes, produced residual flexibility values with errors in the 0.4–2.5% range. The errors were determined by comparing the residual terms of the test data to the residual terms generated from a mathematical model that was correlated to the exact theoretical solution.

The curve fitting process was also applied to a frame structure that simulates a space shuttle cargo pallet, which is more complex than a straight beam. The residual flexibility values for the pallet simulator, retaining the first eight elastic modes, were found to be in the 0.6–4.0% range. A theoretical solution is not available for the frame structure. The exact answer was generated by correlating the mathematical model to all the elastic natural frequencies and mode shapes up to the first bending mode of the trunnion (i.e., 14 elastic modes).

The development of the weighted curve fit of the residual function has made possible further investigation of the residual flexibility modal testing technique. Additional studies are needed in the area of modal parameter estimation (damping evaluation), because this is the cause of the irregular data in the residual function. The next step, which is also under investigation, is how to use the residual terms to accurately correlate a mathematical model.

REFERENCES

Admire, J. R., Ivey, E. W., and Tinker, M. L., 1992a, "Mass-Additive Modal Test Method for Verification of Constrained Structural Models," *Proceedings of the 10th International Modal Analysis Conference*, pp. 312–318.

Admire, J. R., Tinker, M. L., and Ivey, E. W., 1992b, "Residual Flexibility Test Method for Verification of Constrained Structural Models," *Proceedings of the 33rd Structures, Structural Dynamics and Materials Conference*, pp. 1614–1622.

Blevins, R. D., 1979, *Formulas for Natural Frequency and Mode Shape*, Van Nostrand Reinhold Company, New York.

Bookout, P. S., 1993, "Statistically Generated Weighted Curve Fit of Residual Functions," *Proceedings of the 64th Shock and Vibration Symposium*, Vol. I, pp. 422–431.

Coleman, A. D., 1988, "A Mass Additive Technique for Modal Testing as Applied to the Space Shuttle ASTRO-1 Payload," *Proceedings of the 6th International Modal Analysis Conference*, pp. 154–159.

Craig, R. R., and Bampton, M. C. C., 1968, "Coupling of Substructures for Dynamic Analyses," *AIAA Journal*, Vol. 6, No. 7, pp. 1313–1319.

Klosterman, A. L., and Lemon, J. R., 1972, "Dynamic Design Analysis Via the Building Block Approach," *Shock and Vibration Bulletin*, No. 42, Pt. 1, pp. 97–104.

MacNeal, R. H., 1971, "A Hybrid Method of Component Mode Synthesis," *Computers and Structures*, Vol. 1, pp. 581–601.

Martinez, D. R., Carne, T. G., and Miller, A. K., 1984, "Combined Experimental/Analytical Modeling Using Component Mode Synthesis," *Proceedings of the 25th Structures, Structural Dynamics and Materials Conference*, pp. 140–152.

Miller, I. R., Freund, J. E., and Johnson, R., 1990, *Probability and Statistics for Engineers*, Prentice–Hall, Englewood Cliffs, NJ.

Rubin, S., 1975, "Improved Component Mode Representation for Structural Dynamic Analysis," *AIAA Journal*, Vol. 13, pp. 995–1006.

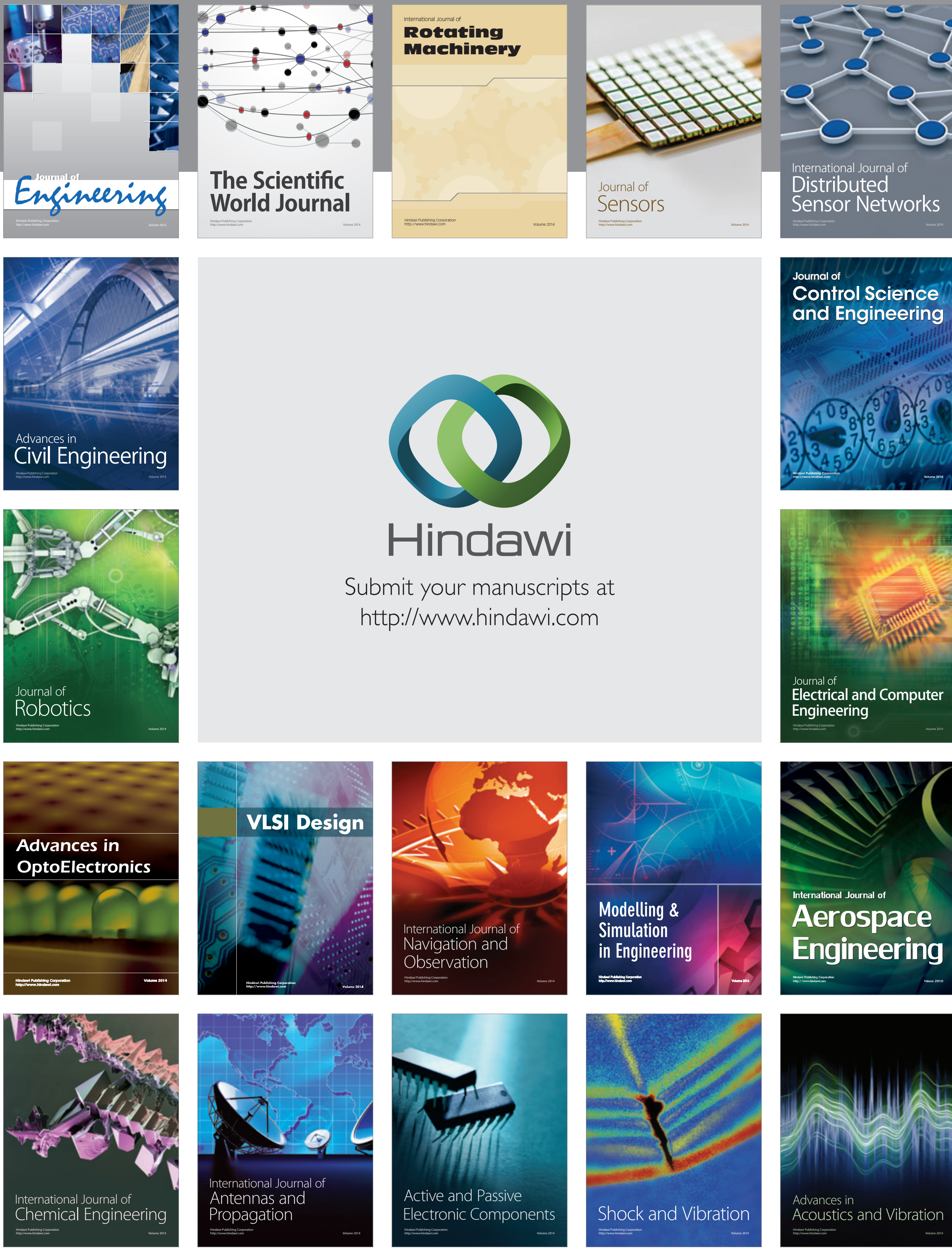
Journal of
Engineering
The Scientific World Journal
International Journal of
Rotating Machinery
Journal of
Sensors
International Journal of
Distributed Sensor Networks
Advances in
Civil Engineering
Journal of
Control Science and Engineering
Hindawi
Submit your manuscripts at
http://www.hindawi.com
Journal of
Robotics
Journal of
Electrical and Computer Engineering
Advances in
OptoElectronics
VLSI Design
International Journal of
Navigation and Observation
Modelling & Simulation in Engineering
International Journal of
Aerospace Engineering
International Journal of
Chemical Engineering
International Journal of
Antennas and Propagation
Active and Passive Electronic Components
Shock and Vibration
Advances in
Acoustics and Vibration